SF2A 2011
G. Alecian, K. Belkacem, R. Samadi and D. Valls-Gabaud (eds)

NONLINEAR SIMULATIONS OF THE CONVECTION-PULSATION COUPLING

T. Gastine[1] and B. Dintrans[2]

Abstract. In cold Cepheids close to the red edge of the classical instability strip, a strong coupling between the stellar pulsations and the surface convective motions occurs. This coupling is by now poorly described by 1-D models of convection, the so-called "time-dependent convection models" (TDC). The intrinsic weakness of such models comes from the large number of unconstrained free parameters entering in the description of turbulent convection. A way to overcome these limits is to compute two-dimensional direct simulations (DNS), in which all the nonlinearities are correctly solved. Two-dimensional DNS of the convection-pulsation coupling are presented here. In an appropriate parameter regime, convective motions can actually quench the radial pulsations of the star, as suspected in Cepheids close to the red edge of the instability strip. These nonlinear simulations can also be used to determine the limits and the relevance of the TDC models.

Keywords: Convection , Instabilities , Stars: oscillations , Methods: numerical , Stars: Variables: Cepheids

1 Introduction

The cold Cepheids located close to the red edge of the classical instability strip have a large surface convective zone that affects their pulsation properties (e.g. the reviews of Gautschy & Saio 1996; Buchler 2009). The first calculations, that assumed *frozen-in* convection, predicted a cooler red edge than the observed one. Indeed, as already stated by Baker & Kippenhahn (1965), a non-adiabatic treatment of the convection-pulsation coupling is mandatory to predict the red edge location with a better accuracy.

Several time-dependent convection (TDC) models were therefore developed to address this coupling (e.g. Stellingwerf 1982; Kuhfuß 1986; Xiong 1989) and succeeded in reproducing the correct location of the red edge, despite their disagreements with the physical origin of the mode stabilisation (e.g. Bono et al. 1999; Yecko et al. 1998; Grigahcène et al. 2005).

However, all these formulations involve many free and degenerate parameters (e.g. the seven dimensionless α coefficients used by Yecko et al. 1998) that are either fitted to the observations or hardly constrained by theoretical values. Nevertheless, another way to tackle this problem is to compute 2-D and 3-D direct numerical simulations (DNS) that correctly take into account the nonlinearities involved in this coupling. Results of such pioneering 2-D nonlinear simulations of the convection-pulsation coupling are presented in the following.

2 The convection-pulsation coupling

Our system corresponds to a local zoom around an ionisation region responsible for the driving of the acoustic modes excited by the κ-mechanism. It is composed of a 2-D cartesian layer filled with a monatomic and perfect gas. The opacity bump associated with this ionisation zone is modelled by a temperature-dependent radiative conductivity profile $K(T)$ (for further details, see Gastine & Dintrans 2008a). In addition to the κ-mechanism, the conductivity profile is deep enough to locally get a superadiabatic temperature gradient, meaning that convective motions develop there, according to Schwarzschild's criterion. A strong coupling between convection and the acoustic oscillations therefore develops.

The hydrodynamical equations are then advanced in time with the high-order, finite-difference pencil code*, which is fully explicit except for the radiative diffusion term that is solved implicitly thanks to a parallel alternate

[1] Max-Planck-Institut für Sonnensystemforschung, Max-Planck-Strasse 2, 37191 Katlenburg-Lindau, Germany
[2] Institut de Recherche en Astrophysique et Planétologie, CNRS/Université de Toulouse, 14 Av. Edouard Belin, 31400 Toulouse, France
*See `http://www.nordita.org/software/pencil-code/` and Brandenburg & Dobler (2002).

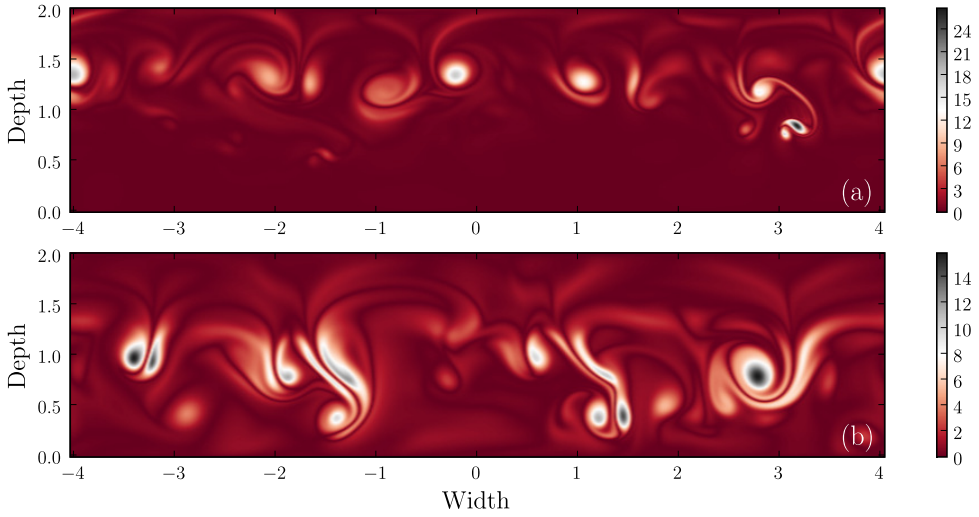

Fig. 1. Snapshot of the modulus of the vorticity field $|\vec{\nabla} \times \vec{u}|$ in the G8 (**a**) and in the G8H8 simulations (**b**).

direction implicit (ADI) solver (Gastine & Dintrans 2008a). The simulation box spans about 10% of the star radius around the ionisation region. In order to ensure that both thermal relaxation and nonlinear saturation of the κ-mechanism are achieved, the simulations are computed over more than 4000 days (corresponding roughly to 1500 periods of oscillation, see Gastine & Dintrans 2011a).

Figure 1 displays a snapshot of the vorticity field for two simulations discussed in (Gastine & Dintrans 2011a), namely G8 (upper panel) and G8H8 (lower panel). This vorticity field highlights the convective motions that are approximately localised in the middle of the layer, where the radiative conductivity is minimum. Differences in the typical length-scale of convection are noticeable between these two DNS: convective eddies are smaller scale in the G8 simulation than in the G8H8 one. Accordingly, the overshooting of convective elements into the lower stably stratified layer is also more pronounced in the latter simulation.

Beyond these qualitative differences, a good way to compare these simulations is to study the temporal evolution of average quantities, such as the vertical mass flux ρu_z. Indeed, as we are considering simulations with both convective motions and oscillations of acoustic modes, it is relevant to use a simple diagnostic that roughly separates their relative contributions. Because the convective plumes have both ascending and descending motions, the average vertical mass flux filters out their contribution and is therefore a good proxy of the amplitude of the acoustic modes. The left panel of Fig. 2 therefore displays the temporal evolution of ρu_z for the two simulations discussed before. An oscillatory behaviour is observed in both cases due to the radial oscillations of the fundamental acoustic mode excited by κ-mechanism. In the G8 simulation, the amplitude first grows exponentially until reaching the nonlinear saturation regime. At first glance, this time evolution looks very similar to what has been already observed in purely radiative simulations of Gastine & Dintrans (2008b), that is, a linear growth of the amplitude and a saturation at a well-defined value. In contrast, the dynamics of the G8H8 simulation differ radically from the previous one as the amplitude remains weak and is highly modulated over time. No clear nonlinear saturation is observed in this case, meaning that the acoustic oscillations are more influenced by convective motions than in the previous DNS.

To separate more precisely the relative contributions of the acoustic modes and the convective motions to the energy budget, the velocity field of each simulations is projected onto an acoustic subspace built from normal eigenmodes (see Bogdan et al. 1993). Thanks to this formalism, it is possible to extract the time evolution of the kinetic energy contained in each acoustic mode found in the nonlinear simulation. The right panel of Fig. 2 displays the time evolution of the energy contained in the fundamental acoustic mode normalised by the total kinetic energy. In the G8 simulation, the acoustic energy linearly increases until its nonlinear saturation, in a similar way to what has been previously observed with the time evolution of ρu_z. Once this saturation is reached, 70% of the kinetic energy is contained in the radial oscillations of the fundamental acoustic mode, while the remaining is in the convective plumes. In other words, the acoustic oscillations are not affected much by the convective motions in this simulation. In contrast, this acoustic energy ratio remains very weak in the

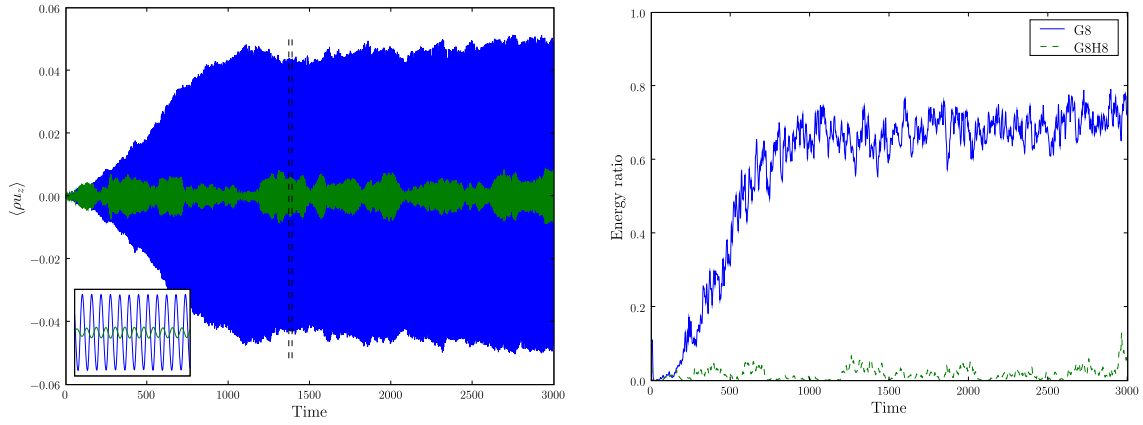

Fig. 2. *Left panel:* Temporal evolution of the mean vertical mass flux ρu_z for the two simulations G8 (solid blue line) and G8H8 (solid green line). The two vertical dashed black lines define the boundaries of the zoom displayed in the bottom left corner. *Right panel:* temporal evolution of the energy contained in acoustic modes normalised by the total kinetic energy for the two simulations G8 (solid blue line) and G8H8 (dashed green line).

other simulation. Despite some transient increases during which non-trifling values ($\simeq 10\%$) are obtained, the average ratio is less than 5%, and convective motions contains the bulk of the kinetic energy. In this case, the radial oscillations excited by the κ-mechanism are thus quenched by convective plumes. This situation is relevant to the physics of Cepheids close to the red edge of the instability strip, where the unstable acoustic modes are supposed to be damped by the surface convective motions. This convective quenching of the acoustic oscillations may be the direct signature of the different density contrasts in the G8 and the G8H8 simulations: in fact, weaker stratification (as in G8H8) leads to bigger vortices (see Fig. 1b), meaning that the energy is contained in larger convective structures. In our DNS, the amplitue of the κ-mechanism seems to be controlled by the screening effect due to these large convective vortices (Gastine & Dintrans 2011a).

3 Limits of time-dependent convection models

The nonlinear simulations of the convection-pulsation coupling, where the acoustic modes strongly modulate the convective motions over time (as in the G8 simulation) are also good candidates to test and compare the relevance of different prescriptions of 1-D time-dependent convection (TDC) models. We focus here on two popular formulations widely used in Cepheids models, namely the TDC model of Stellingwerf (1982) and the one of Kuhfuß (1986). In these formulations, a single equation for the turbulent kinetic energy $\mathcal{E}_t$ is added to the classical mean-field equations and the main second-order correlations, such as the convective flux, are expressed as a function of $\mathcal{E}_t$ only:

$$\begin{cases} \mathcal{F}_{\rm St}(z,t) = \alpha_{\rm St}\dfrac{A}{B}\mathcal{E}_t\,\mathrm{sign}(\nabla-\nabla_{\rm ad})\sqrt{|\nabla-\nabla_{\rm ad}|}, \\ \mathcal{F}_{\rm Ku}(z,t) = \alpha_{\rm Ku}A\sqrt{\mathcal{E}_t}\,(\nabla-\nabla_{\rm ad})\,, \end{cases} \tag{3.1}$$

where $\nabla = d\ln T/d\ln p$, $\nabla_{\rm ad} = 1 - c_v/c_p$ and

$$\mathcal{E}_t(z,t) = \left\langle \frac{{u_z'}^2}{2} \right\rangle, \quad A = c_p\,\langle\rho\rangle\,\langle T\rangle \quad \text{and} \quad B = \sqrt{c_p\,\langle T\rangle\,\nabla_{\rm ad}}, \tag{3.2}$$

where p is the pressure, ρ the density, and the brackets denote a horizontal average. Each of these two TDC expressions thus involves one dimensionless parameter ($\alpha_{\rm St}$ and $\alpha_{\rm Ku}$, respectively) that is poorly constrained by theory (Yecko et al. 1998). The nonlinear results of the G8 simulations are compared to these TDC recipes by computing χ^2-statistics to extract the optimum α coefficients corresponding to each formulation.

Figure 3 compares the convective flux in the DNS with the two TDC prescriptions computed with the best fit values $\alpha_{\rm St}$ and $\alpha_{\rm Ku}$ obtained in (Gastine & Dintrans 2011b). Stellingwerf's formulation seems to give a better agreement with the nonlinear simulation than Kuhfuß's one. Indeed, the Kuhfuß model overestimates

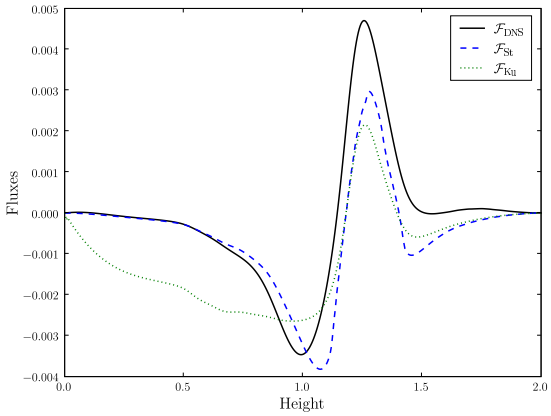

Fig. 3. Mean convective flux in the G8 simulation (solid black line), compared with the best TDC predictions based on the models of Stellingwerf (dashed blue line) and Kuhfuß (dotted green line).

the overshooting as the (negative) convective flux remains non-negligible until the bottom of the radiative zone. In contrast, the Stellingwerf profile accounts for the local penetration of convective plumes better and shows the same exponential-like decay in the negative convective flux when sinking in the radiative zone. However, the two models are fairly similar in the bulk of the convective zone, where convection is fully developed. One also notes that they both predict a negative flux at the top of the convective zone, which is an upper overshooting of convective motions near the surface that is not observed in the DNS.

4 Conclusion

The main weakness of all theories of 1-D time-dependent convection lies in the large number of free parameters involved in the description of convection. New constraints must therefore be found to reduce the intrinsic degeneracy of these models and to check the relevance of the different assumptions underlying these parametrisations.

Nonlinear 2-D direct numerical simulations are a useful way to address the convection-pulsation coupling that occurs in cold Cepheids. These simulations show a variable influence of convection onto the acoustic modes excited by κ-mechanism: (*i*) either the amplitude of the acoustic modes remains very weak and convective motions quench the oscillations ; (*ii*) or the kinetic energy is mainly contained in the acoustic modes and convective plumes are strongly modulated over time by the radial oscillations. While the former situation is relevant to the stabilisation of the oscillations of Cepheids close to to the red edge, the latter is a good candidate to draw the limits of current TDC recipes. Focusing on two such widely used models, Stellingwerf's formulation is found to give a better agreement with the nonlinear results than does Kuhfuß's.

This first comparison of TDC with nonlinear 2-D simulations emphasises how DNS can be helpful to validate and improve the future 1-D models of convection.

This work was granted access to the HPC resources of CALMIP under the allocation 2010-P1021 (`http://www.calmip.cict.fr`).

References

Baker, N. & Kippenhahn, R. 1965, ApJ, 142, 868

Bogdan, T. J., Cattaneo, F., & Malagoli, A. 1993, ApJ, 407, 316

Bono, G., Marconi, M., & Stellingwerf, R. F. 1999, ApJS, 122, 167

Brandenburg, A. & Dobler, W. 2002, CoPhC, 147, 471

Buchler, J. R. 2009, in American Institute of Physics Conference Series, Vol. 1170, American Institute of Physics Conference Series, ed. J. A. Guzik & P. A. Bradley, 51–58

Gastine, T. & Dintrans, B. 2008a, A&A, 484, 29

Gastine, T. & Dintrans, B. 2008b, A&A, 490, 743

Gastine, T. & Dintrans, B. 2011a, A&A, 528, A6

Gastine, T. & Dintrans, B. 2011b, A&A, 530, L7

Gautschy, A. & Saio, H. 1996, ARA&A, 34, 551
Grigahcène, A., Dupret, M.-A., Gabriel, M., Garrido, R., & Scuflaire, R. 2005, A&A, 434, 1055
Kuhfuß, R. 1986, A&A, 160, 116
Stellingwerf, R. F. 1982, ApJ, 262, 330
Xiong, D. 1989, A&A, 209, 126
Yecko, P. A., Kolláth, Z., & Buchler, J. R. 1998, A&A, 336, 553